frontiers | Frontiers in Physics

TYPE Original Research
PUBLISHED 18 September 2024
DOI 10.3389/fphy.2024.1468722

Check for updates

OPEN ACCESS

EDITED BY
Jingsong Li,
Anhui University, China

REVIEWED BY
Chaitanya Kumar Suddapalli,
Tata Institute of Fundamental Research (Hyderabad), India
Hongli Wang,
North University of China, China
Linguang Xu,
Anhui Polytechnic University, China

*CORRESPONDENCE
Yong-Liang Li,
✉ liyongliang1973@163.com

RECEIVED 22 July 2024
ACCEPTED 06 September 2024
PUBLISHED 18 September 2024

CITATION
Yu H, Chen C and Li Y-L (2024) Tunable continuous wave Yb:CaWO$_4$ laser operating in NIR spectral region.
Front. Phys. 12:1468722.
doi: 10.3389/fphy.2024.1468722

Tunable continuous wave Yb:CaWO$_4$ laser operating in NIR spectral region

Hao Yu, Chong Chen and Yong-Liang Li*

School of Opto-electronics Engineering, Changchun University of Science and Technology, Changchun, Jilin, China

A tunable continuous wave (CW) Yb:CaWO$_4$ laser operating in near infrared (NIR) spectral region is demonstrated by pumping with a diode laser. Continuously broadband tunable wavelengths are obtained in two polarizations by rotating the Lyot filter. The tuning widths of the output wavelengths in the π- and σ-polarizations are 42 nm (from 1005.2 nm to 1047.2 nm) and 41.8 nm (from 1005.1 nm to 1046.9 nm), respectively. At an absorbed pump power of 15.6 W at 976 nm, the maximum output powers in the π- and σ-polarizations are 5.2 W at 1026.2 nm and 4.7 W at 1028.1 nm, respectively. To the best of our knowledge, this is the first tunable laser operation by using Yb:CaWO$_4$ crystal.

KEYWORDS

diode-pumped, solid-state laser, tunable, Yb:CaWO$_4$, Lyot filter

1 Introduction

Trivalent ytterbium ions (Yb^{3+})-doped crystals have been considered one of the most promising active medium for solid-state lasers because it has a small quantum defect, a simple two-manifold structure, a low thermal load, a longer energy-storage lifetime, no upconversion and cross relaxation processes and excited state absorption compared to trivalent neodymium ions (Nd^{3+}) [1–5]. Yb^{3+}-doped tungstates such as Yb:NaY(WO$_4$)$_2$ [6–10], Yb:NaGd(WO$_4$)$_2$ [11–14], NaLu(WO$_4$)$_2$ [15], Yb:NaLa(WO$_4$)$_2$ [16–18] and Yb:KLu(WO$_4$)$_2$ [19–21] have played an important role in the development of solid-state lasers due to the broader emission and absorption linewidths. Yb^{3+}-doped calcium tungstate (CaWO$_4$) crystal as an excellent host medium for rare-earth ions, has been widely used in solid-state lasers. Recently, the absorption and emission spectra of Yb:CaWO$_4$ crystal and its CW lasing properties have been investigated [22–24]. The absorption spectra of the Yb:CaWO$_4$ crystal from 875 nm to 1075 nm in two polarizatios were carried out in a UV-Vis-IR absorption spectrophotometer (Cary 5000, VARIAN USA). The emission spectra of the Yb:CaWO$_4$ crystal from 875 nm to 1075 nm in two polarizatios were measured at 875–1075 nm by a steady-state time-resolved fluorescence spectrometer (FLS-980, Edinburgh England) under 976 nm. The emission cross-sections can be calculated from the measured fluorescence spectra by the Füchtbauer-Landenburg equation [25]

$$\sigma(\lambda) = \frac{\lambda^5 \cdot I(\lambda)}{8\pi n^2 c\tau_r I(\lambda) d\lambda} \tag{1}$$

where λ is the wavelength, $I(\lambda)$ is the fluorescence intensity, $n = 1.91$ [26] is the refractive index of the Yb:CaWO$_4$ crystal, c is the velocity of light, $\tau_r = \tau_f = 428$ μs [22], τ_r and τ_f are the radiative lifetime and the fluorescence lifetime, respectively. Calculate using Equation 1, the cross-section curve is shown in Figure 1. It can be seen that there were three absorption peaks in π-polarization, which were 965, 976 and 994 nm respectively, and the corresponding absorption

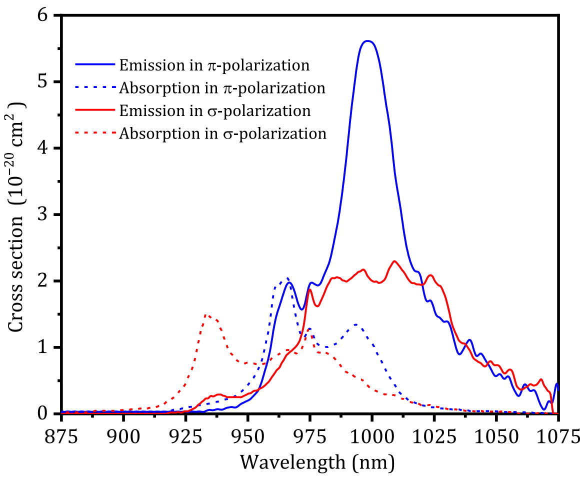

FIGURE 1
Absorption and emission cross-sections of the Yb:CaWO$_4$ crystal from 875 to 1075 nm.

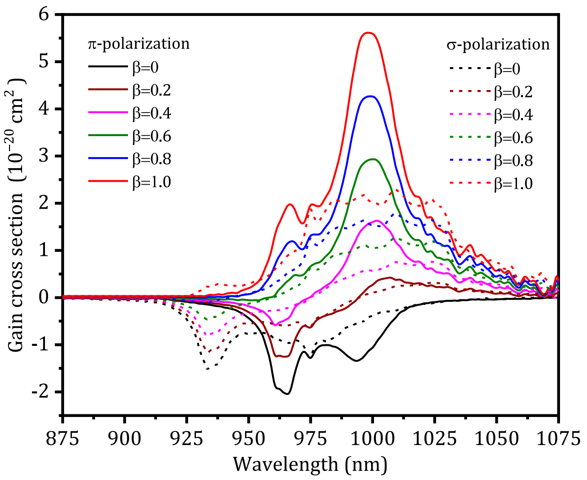

FIGURE 2
Gain cross-sections of the Yb:CaWO$_4$ crystal from 875 to 1075 nm.

cross-sections ($\sigma_{abs,\pi}$) were 2.03, 1.28 and 1.34 × 10^{-20} cm^2 respectively. Two absorption peaks in σ-polarization were 934 and 975 nm, respectively, and the corresponding absorption cross-sections ($\sigma_{abs,\sigma}$) were 1.48 and 1.27 × 10^{-20} cm^2 respectively. Two emission peaks in π-polarization were 967 and 997 nm respectively, and the corresponding emission cross-sections ($\sigma_{em,\pi}$) were 1.97 and 5.61 × 10^{-20} cm^2 respectively. There was a wide emission spectrum (from 976 to 1024 nm) in σ-polarization, and corresponding to an emission cross-section ($\sigma_{em,\sigma}$) of about 2.0 × 10^{-20} cm^2. The gain cross-sections of the Yb:CaWO$_4$ crystal from 875 nm to 1075 nm in two polarizations were calculated by $\sigma_{g,i} = \beta\sigma_{em,i} - (1-\beta)\sigma_{abs,i}$ [27], where β is the fraction of Yb^{3+} excited to the upper state, and $i = \pi, \sigma$ represents the π- and σ-polarization respectively, as shown in Figure 2. It can be seen from Figure 2 that the Yb:CaWO$_4$ crystal had a wide gain spectrum in both directions, which made it suitable for tunable laser output. In this work, we realized the first tunable Yb:CaWO$_4$ laser in NIR spectral range. The laser tuning ranges in π- and σ-polarizations were 42 nm and 41.8 nm, respectively. Continuously broadband tunable wavelengths are obtained in two polarizations by rotating the Lyot filter, which have the potential applications in some fields, such as mid-infrared laser absorption spectroscopy [28], wavelength modulation spectroscopy [29] and photoacoustic spectroscopy [30], etc.

2 Experimental setup

A schematic setup for the diode-pumped tunable Yb:CaWO$_4$ laser is shown in Figure 3. In our experiment, we used a 9 mm long Yb:CaWO$_4$ was crystal with a doping concentration of 1.2 at% Yb^{3+}, which supplied by Fujian Institute of Material Structure, Chinese Academy of Sciences. The thermal effect of the laser crystal will affect the spectral width of the tunable Yb:CaWO$_4$ laser, because the increase of the Yb:CaWO$_4$ crystal temperature will lead to changes in the refractive index and absorption coefficient of the crystal, which will directly affect the output spectral characteristics of the laser. The narrower the spectral line width, the higher the output power will be, because the narrower the spectral line, the lower the intracavity loss, the higher the photon number density, the higher the output power. Therefore, in order to reduce the thermal effect of the Yb:CaWO$_4$ crystal, we choose the Yb:CaWO$_4$ crystal with low doping concentration of Yb^{3+}, which can reduce the probability of possible nonradiative cross-relaxation processes and the reabsorption of the laser emission. The Yb:CaWO$_4$ crystal was wrapped in indium foil and mounted on water-cooled copper blocks. The temperature of the water was controlled at 15°C. The pump source of the tunable Yb:CaWO$_4$ laser is a diode array with fiber-coupled output, a maximum output power of 20 W and a radius of the pump beam waist of 200 μm. The two identical convex lenses with the focal length of 150 mm, L_1 and L_2, coupled the pump beam to the Yb:CaWO$_4$ crystal, which were antireflection (AR) coated at 976 nm. The plane mirror (M$_1$) was the input mirror, which was AR coated at 976 nm and high reflectivity (HR) coated at 1000–1050 nm. The concave mirror (M$_2$) with the radius of curvature of −150 mm was the output mirror, which was with a transmittance of about 3.0% at 1000–1050 nm. The concave mirror (M$_3$) with the radius of curvature of −300 mm was the reflector, which were HR coated at 1000–1050 nm. To achieve wavelength tuning, a Lyot filter (quartz crystal, thickness d = 2 mm) was inserted into the cavity, which was AR coated at 1000–1050 nm and was which supplied by Jiangyin Yunxiang Optoelectronic Technology Co. , Ltd, China. Figures 3A, B are Lyot filter placed in the π- and σ-polarization, respectively.

3 Results and discussion

The transmittance of Lyot filter, T, can be written as [31]:

$$T = 1 - 4\cot^2\gamma\tan^2\theta\left(1 - \cot^2\gamma\tan^2\theta\right)\sin^2(\delta/2) \qquad (2)$$

$$\cos\alpha = \frac{\cos\gamma - \sin\theta\sin\varphi}{\cos\theta\cos\varphi} \qquad (3)$$

where γ is angle between the internal ray and the optic axis, θ is incident angle ($\theta = \theta_B = 57.2°$ in the experiment), β is angle between the crystal axis and the surface of Lyot filter ($\varphi = 0$ in the experiment), $\delta = 2\pi d(n_o - n_e)\sin^2\gamma/\lambda\sin\theta$ is the optical phase difference. According to

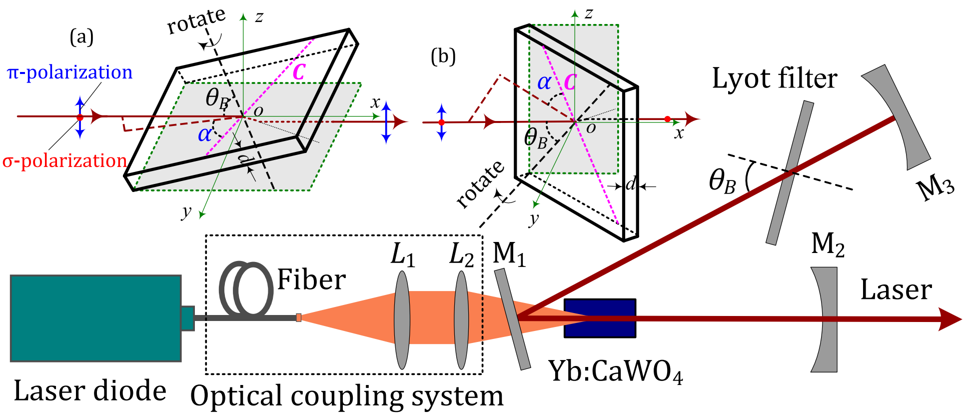

FIGURE 3
Schematic setup for the laser experiment. **(A)** Continuous tuning laser of π-polarization. **(B)** Continuous tuning laser of σ-polarization. θ_B is Brewster's angle, *C* is the crystal axis, which is parallel to the surface of the crystal, α is the angle between the projection of the incident ray on the surface of the crystal and the crystal axis, *d* is the thickness of the crystal.

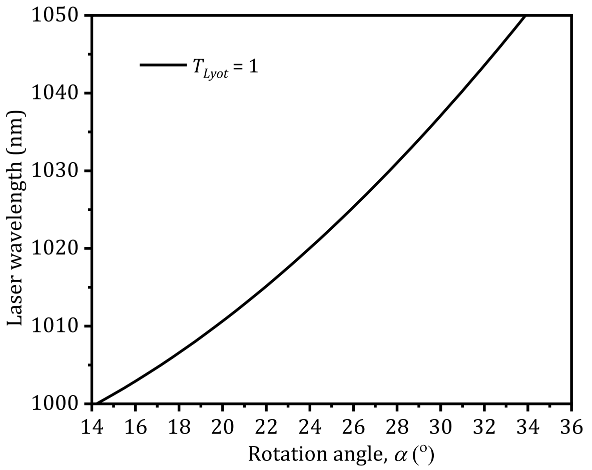

FIGURE 4
Laser wavelength *versus* rotation angle at *T* = 1.

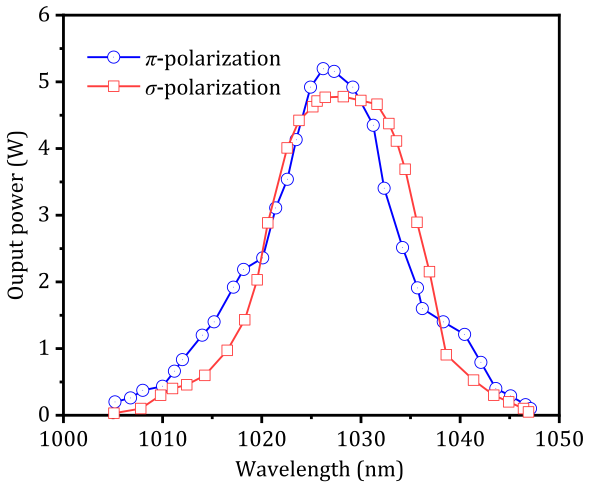

FIGURE 5
Output powers of two polarization directions *versus* laser output wavelength.

Equations 2, 3, the angle, α (rotation angle) is changed by rotating the Lyot filter, the transmittance of Lyot filter, *T*, is also changed. Therefore, by rotating the Lyot filter, we could change its transmittance to different wavelengths in the NIR region, resulting in the continuously tunable laser output. The relationship between the rotation angle and the laser wavelength is calculated (*T* = 1), as shown in Figure 4. As can be seen from Figure 4, the different rotation angle, α, corresponds to different laser wavelength (the maximum transmittance, *T* = 1), thus the corresponding tunable wavelength output can be realized.

At an absorbed pump power of 15.6 W (or an incident pump power of 20 W), the output powers of the Yb:CaWO$_4$ laser for output wavelengths in the π-polarization are shown in Figure 5. As can be seen from Figure 5, the peak power is 5.2 W at 1026.2 nm in the π-polarization. The input-output performance of the CW 1026.2 nm Yb:CaWO$_4$ laser is shown in Figure 6. The oscillation threshold is 0.52 W. The slope efficiency and the optical-to-optical efficiency with respect to the absorbed pump power are 34.6% and 33.3%, respectively. The quality factor of the laser beam M^2 = 1.21. The stability of the output power is about 3.2% in 1 h. Using a LABRAM-UV spectrum analyzer to scan the output beam and dealing with the data with software, the tuning spectra of the Yb:CaWO$_4$ laser at the absorbed pump power of 15.6 W is shown in Figure 7. As can be seen from Figure 7, the Yb:CaWO$_4$ laser realized tuning wavelength from 1005.2 nm to 1047.2 nm in the π-polarization. The width of wavelength tuning in the NIR spectral range reached 42 nm.

Similarly, at an absorbed pump power of 15.6 W, the output powers of the Yb:CaWO$_4$ laser in σ-polarization are also shown in Figure 5. As can be seen from Figure 6, the peak power is 4.7 W at 1028.1 nm in the σ-polarization. The input-output performance of the CW 1028.1 nm Yb:CaWO$_4$ laser is also shown in Figure 6. The oscillation threshold is 0.67 W. The slope efficiency and the optical-to-optical efficiency with respect to the absorbed pump power are 30.3% and 30.1%, respectively. The quality factor of the laser beam M^2 = 1.26. The stability of the output power is about 2.7% in 1 h. The spectra of the

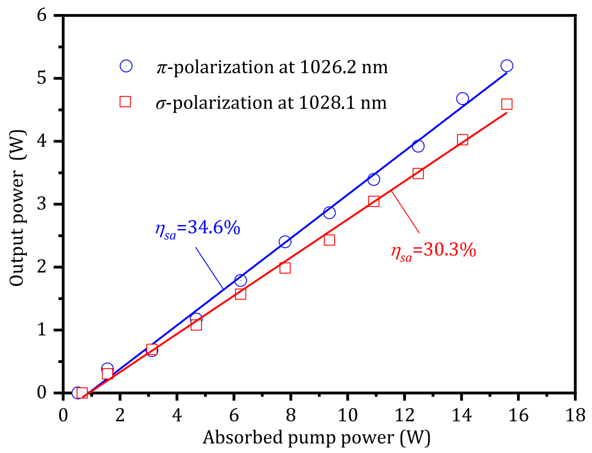

FIGURE 6
Output power at 1026.2 nm and 1028.1 nm *versus* absorbed pump power.

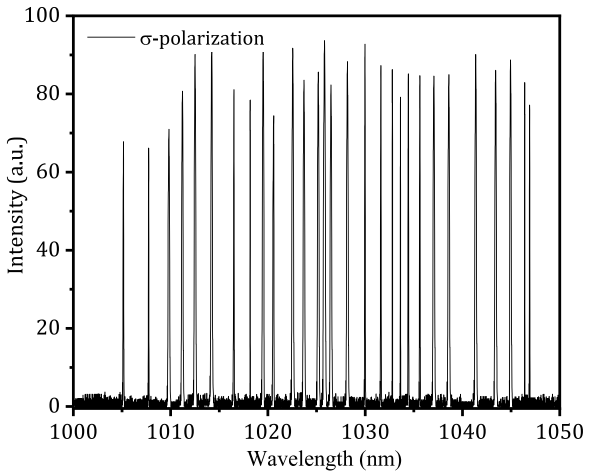

FIGURE 8
Spectra of the Yb:CaWO$_4$ laser from 1005 nm to 1047 nm in the σ-polarization.

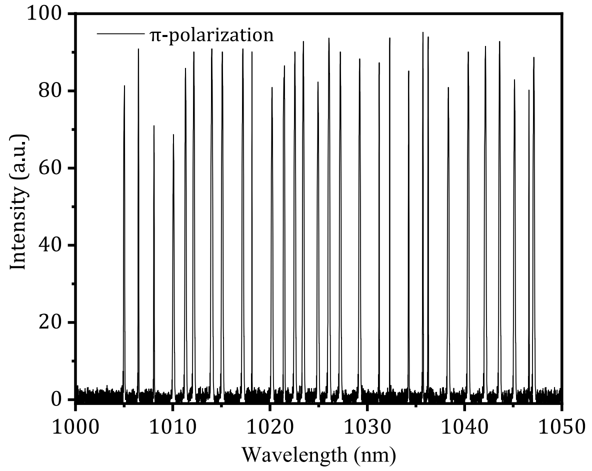

FIGURE 7
Spectra of the Yb:CaWO$_4$ laser from 1005 nm to 1047 nm in the π-polarization.

Yb:CaWO$_4$ laser at the absorbed pump power of 15.6 W is shown in Figure 8. As can be seen from Figure 8, the Yb:CaWO$_4$ laser realized tuning wavelength from 1005.1 nm to 1046.9 nm in the *σ*-polarization. The width of wavelength tuning in the NIR spectral range reached 41.8 nm. At the highest output power, the output beam profile of each tuned wavelength in both polarized directions was measured, which exhibited almost Gaussian distribution along both axes.

4 Conclusion

In conclusion, we first demonstrate a diode pumped continuously tunable Yb:CaWO$_4$ laser in NIR spectral regions. The tuning widths of the output wavelengths in the π- and σ-polarizations are 42 nm (from 1005.2 nm to 1047.2 nm) and 41.8 nm (from 1005.1 nm to 1069.9 nm), respectively. Continuously broadband tunable wavelengths are obtained in two polarizations by rotating the Lyot filter, respectively. At an absorbed pump power of 15.6 W at 976 nm, the maximum output powers in the π- and σ-polarization are 5.2 W at 1026.2 nm and 4.7 W at 1028.1 nm, respectively. To the best of our knowledge, this is the first tunable laser operation by using Yb:CaWO$_4$ crystal. We believe that the same technology can be applied to other Yb^{3+}-doped tungstate crystals to realize tunable laser output.

Data availability statement

The raw data supporting the conclusions of this article will be made available by the authors, without undue reservation.

Author contributions

HY: Writing–original draft, Writing–review and editing. CC: Writing–original draft, Writing–review and editing. Yong Liang Y-LL: Writing–original draft, Writing–review and editing.

Funding

The author(s) declare that financial support was received for the research, authorship, and/or publication of this article. This work is supported by the Natural Science Foundation of China (Grant No. 62075018), People's Government of Jilin Province (Grant No. 20200403018SF).

Conflict of interest

The authors declare that the research was conducted in the absence of any commercial or financial relationships that could be construed as a potential conflict of interest.

Publisher's note

References

1. Mougel F, Dardenne K, Aka G, Kahn-Harari A, Vivien D. Ytterbium-doped $Ca_4GdO(BO_3)_3$: an efficient infrared laser and self-frequency doubling crystal. *J Opt Soc Am B* (1999) 16:164–72. doi:10.1364/josab.16.000164

2. Xia J, Liu H, Hu Z, Yang R, Lü Y, Jiang Z, et al. Pure-three-level Yb:GdCOB CW laser at 976nm. *Opt Lett* (2018) 43:3981–4. doi:10.1364/ol.43.003981

3. Zhu K, Zhou H, Wang J, Qiu J, Ye L, Zhang J, et al. Optical temperature sensing characteristics of Yb^{3+}/Nd^{3+} co-doped YAG single crystal fiber based on up-conversion luminescence. *J Lumin* (2024) 267:120347. doi:10.1016/j.jlumin.2023.120347

4. Sato Y, Arzakantsyan M, Akiyama J, Taira T. Anisotropic Yb:FAP laser ceramics by micro-domain control. *Opt Mater Express* (2014) 4:2006–15. doi:10.1364/ome.4.002006

5. Druon A, Balembois F, Brun A, Mougel F, Aka G, Vivien D. Theoretical and experimental investigations of a diode-pumped quasi-three-level laser: the Yb^{3+}-doped $Ca_4GdO(BO_3)_3$ (Yb:GdCOB) laser. *IEEE J Quant Electron* (2000) 36:598–606. doi:10.1109/3.842102

6. Jie M, Wang J, Shen D, Yu H, Tang D. Dissipative soliton operation of a diode pumped Yb:$NaY(WO_4)_2$ laser. *Opt Express* (2015) 23:32311. doi:10.1364/oe.23.032311

7. Liu J, Zhang H, Wang J, Petrov V. Continuous-wave and Q-switched laser operation of Yb:$NaY(WO_4)_2$ crystal. *Opt Express* (2007) 15:12900–4. doi:10.1364/oe.15.012900

8. Xie G, Tang D, Zhang H, Wang J. Qian L Efficient operation of a diode-pumped Yb:$NaY(WO_4)_2$ laser. *Opt Express* (2008) 16:1686–91. doi:10.1364/oe.16.001686

9. Liu J, Wan Y, Tian X, Dai Q, Han W. Polarization state of a continuous-wave Yb:$NaY(WO_4)_2$ disordered crystal laser. *Laser Phys Lett* (2013) 10:075003. doi:10.1088/1612-2011/10/7/075003

10. Lan R, Pan L, Utkin I, Ren Q, Zhang H, Wang Z, et al. Passively Q-switched Yb^{3+}:$NaY(WO_4)_2$ laser with GaAs saturable absorber. *Opt Express* (2010) 18:4000–5. doi:10.1364/oe.18.004000

11. Liu J, Petrov V, Zhang H, Wang J, Jiang M. Efficient passively Q-switched laser operation of Yb in the disordered $NaGd(WO_4)_2$ crystal host. *Opt Lett* (2007) 32:1728–30. doi:10.1364/ol.32.001728

12. Fan J, Zhang H, Wang J, Ling Z, Xia H, Chen X, et al. Growth, structure and thermal properties of Yb^{3+}-doped $NaGd(WO_4)_2$ crystal. *J Phys D: Appl Phys* (2006) 39:1034–41. doi:10.1088/0022-3727/39/6/007

13. Faure N, Borel C, Couchaud M, Basset G, Templier R, Wyon C. Optical properties and laser performance of neodymium doped scheelites $CaWO_4$ and $NaGd(WO_4)_2$. *Appl Phys B* (1996) 63:593–8. doi:10.1007/bf01830998

14. Rico M, Liu J, Griebner U, Petrov V, Serrano M, Betegón F, et al. Tunable laser operation of ytterbium in disordered single crystals of Yb:$NaGd(WO_4)_2$. *Opt Express* (2004) 12:5362–7. doi:10.1364/opex.12.005362

15. Cortés A, Torres J, Han X, Cascales C, Zaldo C, Mateos X, et al. Tunable continuous wave and femtosecond mode-locked Yb^{3+} laser operation in Yb:$NaLu(WO_4)_2$. *J Appl Phys* (2007) 101:063110. doi:10.1063/1.2490382

16. Liu J, Torres J, Betegón F, Serrano M, Cascales C, Zaldo C, et al. Continuous wave diode-pumped operation of an Yb:$NaLa(WO_4)_2$ laser at room temperature. *Opt Laser Technol* (2007) 39:558–61. doi:10.1016/j.optlastec.2005.10.011

17. Subbotin K, Zharikov E, Smirnov V. Yb-and Er-Doped single crystals of double tungstates $NaGd(WO_4)_2$, $NaLa(WO_4)_2$, and $NaBi(WO_4)_2$ as active media for lasers operating in the 10 and 15 μm ranges. *Opt Spectrosc* (2002) 92:601–8. doi:10.1134/1.1473604

18. Liu J, Torres J, Cascales C, Betegon F, Serrano M, Volkov V, et al. Growth and continuous-wave laser operation of disordered crystals of Yb^{3+}:$NaLa(WO_4)_2$ and Yb^{3+}:$NaLa(MoO_4)_2$. *Physica Status Solidi A, Appl Res* (2005) 202:R29–R31. doi:10.1002/pssa.200510001

19. Cao S, Dong L, Chen J, Han W, Liu J. Efficient acousto-optically Q-switched compact Yb:KLuW laser with self-Raman conversion. *Opt Laser Technol* (2021) 143:107328. doi:10.1016/j.optlastec.2021.107328

20. Liu J, Griebner U, Petrov V, Zhang H, Zhang J, Wang J. Efficient continuous-wave and Q-switched operation of a diode-pumped Yb:$KLu(WO_4)_2$ laser with self-Raman conversion. *Opt Lett* (2005) 30:2427–9. doi:10.1364/ol.30.002427

21. Tian K, Li Y, Yang J, Dou X, Xu H, Han W, et al. Passive Q-switching of an Yb:$KLu(WO_4)_2$ laser with 2D saturable absorbers of MoS_2 and WS_2: scaling the output power to 2-W level. *Opt Commun* (2019) 436:42–6. doi:10.1016/j.optcom.2018.12.009

22. Chen J, Dong L, Liu F, Xu H, Liu J. Investigation of Yb:$CaWO_4$ as a potential new self-Raman laser crystal. *CrystEngComm* (2021) 23:427–35. doi:10.1039/d0ce01538e

23. Dong L, Zhou Y, Chen J, Han W, Zhang Y, Xu H, et al. Lasing properties and their anisotropy of Yb:$CaWO_4$ crystal. *Opt Commun* (2022) 508:127815. doi:10.1016/j.optcom.2021.127815

24. Han W, Dong L, Zhang Y, Xu H, Liu J. Comparative study on passive Q-switching laser properties of Yb:$CaWO_4$ and Yb:$NaY(WO_4)_2$ crystals. *Opt Mater* (2023) 137:113571. doi:10.1016/j.optmat.2023.113571

25. Aull B, Jenssen H. Vibronic interactions in Nd:YAG resulting in nonreciprocity of absorption and stimulated emission cross sections. *IEEE J Quant Electron* (1982) 18:925–30. doi:10.1109/jqe.1982.1071611

26. Thornton J, Fountain W, Flint G, Crow T. Properties of neodymium laser materials. *Appl Opt* (1969) 8:1087–102. doi:10.1364/ao.8.001087

27. DeLoach L, Payne S, Chase L, Smith L, Kway W, Krupke W. Evaluation of absorption and emission properties of Yb^{3+} doped crystals for laser applications. *IEEE J Quant Electron* (1993) 29:1179–91. doi:10.1109/3.214504

28. Li J, Deng H, Sun J, Yu B, Fischer H. Simultaneous atmospheric CO, N_2O and H_2O detection using a singlequantum cascade laser sensor based on dual-spectroscopy technique. *Sens Actuators B: Chem* (2016) 231:723–32. doi:10.1016/j.snb.2016.03.089

29. Xu L, Zhou S, Liu N, Zhang M, Liang J, Li J. Multigas sensing technique based on quartz crystal tuning fork-enhanced laser spectroscopy. *Anal Chem* (2020) 92:14153–63. doi:10.1021/acs.analchem.0c03233

30. Huang Q, Wei Y, Li J. Simultaneous detection of multiple gases using multi-resonance photoacoustic spectroscopy. *Sens Actuators B: Chem* (2022) 369:132234. doi:10.1016/j.snb.2022.132234

31. Wang X, Yao J. Transmitted and tuning characteristics of birefringent filters. *Appl Opt* (1992) 31:4505–7. doi:10.1364/ao.31.004505